The Astronomical Journal, 158:180 (8pp), 2019 November https://doi.org/10.3847/1538-3881/ab3e77

Observation, Modern Light-curve Analysis, and 89 yr Period Study of the Short-period Algol, AE Cassiopeia

Ronald G. Samec[1], Heather Chamberlain[1], Daniel B. Caton[2], and Danny R. Faulkner[3]
[1] Faculty Research Associate, Pisgah Astronomical Research Institute, 1 PARI Drive, Rosman, NC 28772, USA; ronaldsamec@gmail.com
[2] Dark Sky Observatory, Physics and Astronomy Department, Appalachian State University, 525 Rivers Street, Boone, NC 28608-2106, USA; catondb@appstate.edu
[3] Johnson Observatory, 1414 Bur Oak Court, Hebron, KY 41048, USA; drfaulkn@gwm.sc.edu
Received 2019 July 18; revised 2019 August 20; accepted 2019 August 21; published 2019 October 10

Abstract

AE Cas was observed some 40 yr ago by Srivastava & Kandpal and was analyzed by Kopal's Fourier frequency -domain technique. No further precision observations have taken place until the present study, which represents the first modern synthetic analysis of light curves using the 2016 version of the Wilson–Devinney (W–D) Program. It was observed in 2015 October 2, 3 and 23, inclusive, at Dark Sky Observatory in North Carolina with the 0.81 m reflector of Appalachian State University and the 0.9 m reflector at Kitt Peak National Observatory remotely through the Southeastern Association for Research in Astronomy (SARA) consortia. V, R_c, I_c observations were taken. Five times of minimum light were determined from our present observations, which include three primary eclipses and two secondary eclipses. In addition, eight observations at minima were introduced as low weighted times of minimum light from archived All-Sky Automated Survey for Supernovae Variable Star Catalog (ASAS) data and 74 times of minimum light from the literature, some of which were from visual observations. This period study covers an interval of some 89 yr. The period was found to be decaying at a constant rate with a high level of confidence. A VR_cI_c simultaneous W–D Program solution indicates that the system has a mass ratio somewhat less than unity ($q = 0.856 \pm 0.001$), and a component temperature difference of $\sim$2060 K. A q-search was performed and the mass ratio minimized at the above value. The large temperature difference in the components verifies that the binary is not yet in contact. No spots were needed for the solution. The fill-out of our model is 83.2% for the primary component (smaller radius) and 99.1% for the secondary component. So, it is near a classical Algol configuration.

Unified Astronomy Thesaurus concepts: Detached binary stars (375); Stellar evolution (1599); Interacting binary stars (801); Eclipsing binary stars (444); Algol variable stars (24); Contact binary stars (297)

Supporting material: machine-readable tables

1. Introduction

Early analyses of eclipsing binaries prior to the mid 1960s relied on many techniques that were not adequate to physically analyze interacting binaries (Wilson 1994). These included graphical techniques like the Russell Merrill rectified method (Russell & Merrill 1952) and others using spherical and ellipsoidal geometries (i.e., Wood 1971). Many of these early models avoided the physical processes of gravitation and centrifugal force. Kopal's methods (Kopal 1982) included a Fourier analysis frequency-domain approach to the analysis of light curves. Later the potential energy-based methods of modern light-curve analysis were developed, spearheaded by R. E. Wilson & Devinney (Wilson 1994).

Here we present precision photometry and the first modern light-curve analysis of the near-contact system, AE CAS. The first report of these observations was recently given as a poster paper at the American Astronomical Society Meeting #234 (Chamberlain et al. 2019).

2. History

AE Cas was discovered as an Algol by Hoffmeister (1928). Wood & Forbes (1963) presented an ephemeris of

$$\mathrm{HJD} = 2433282.83348\mathrm{d} + 0.75911650E, \quad (1)$$

the Two Micron All Sky Survey (2MASS) gives a $J–K$ of 0.320 ± 0.053 mag, and the AAVSO Photometric All-Sky Survey, first release (APASS-DR1), gives $B–V = 0.53$. Srivastava & Kandpal (1984) presented *UBV* photoelectric observations and analyzed it by a Fourier frequency-domain technique. Three times of minima were presented. The Fourier fit yielded the approximate values, mass ratio $(q) = 0.7$, and inclination $(i) = 80\fdg4$. In the Catalog and AtLas of Eclipsing Binaries (CALEB) database,[4] David Bradstreet gave a binary maker potential-based (uses blackbody atmospheres) fit to these light curves. The results were a semi-detached Algol-type solution which included $\Omega_{1,2}$ (gravitational potentials) = 4.3811 and 3.5856, fill-out$_{1,2}$ = 81% and 100%, $i = 76°$, and $q = 0.9$. Shaw's near-contact binary site[5] gives a magnitude of $V = 12.421$, and the ephemeris

$$\mathrm{JD\ Hel\ Min\ I} = 2451339.6385\mathrm{d} + 0.759135E.$$

as well as a light curve (shown in Figure 1).

This system was observed as a part of our student/professional collaborative studies of interacting binaries using data taken from Dark Sky Observatory (DSO) observations. The observations were taken by R. Samec, D. Caton, and D. Faulkner. Reduction and analyses were done by R. Samec. A survey light curve was taken by the All-Sky Automated Survey for Supernovae (ASAS-SN)[6] Variable Stars Database (The ASAS-SN Catalog of Variable Stars: II; Shappee et al. 2014 and Kochanek et al. 2017) with a $J–K = 0.32$, an ephemeris of

$$\mathrm{JD\ Hel\ MIN\ I} = 2457362.89544 + 0.7591156E, \quad (2)$$

[4] http://caleb.eastern.edu/
[5] http://www.physast.uga.edu/~jss/ncb/
[6] https://asas-sn.osu.edu/

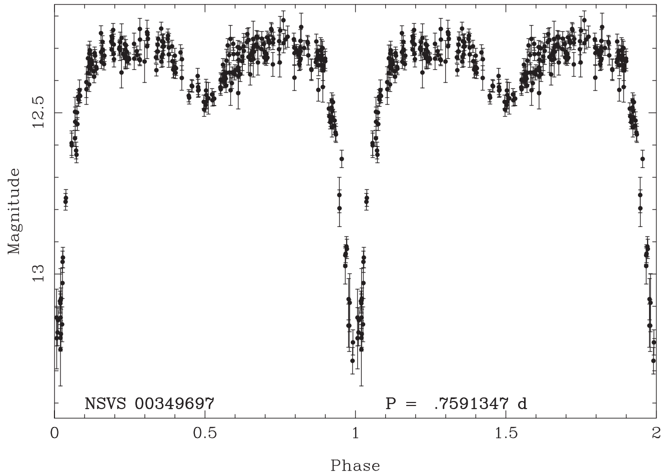

Figure 1. Data from J.S. Shaw's near-contact binaries (http://www.physast.uga.edu/~jss/ncb/LC/lc00349697.pdf).

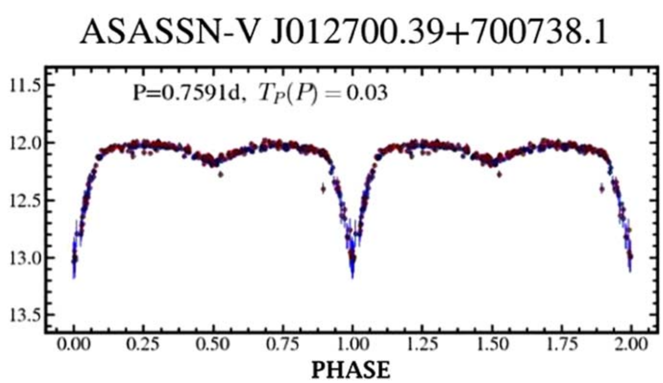

Figure 2. *V* light curves of AE CAS (https://asas-sn.osu.edu/).

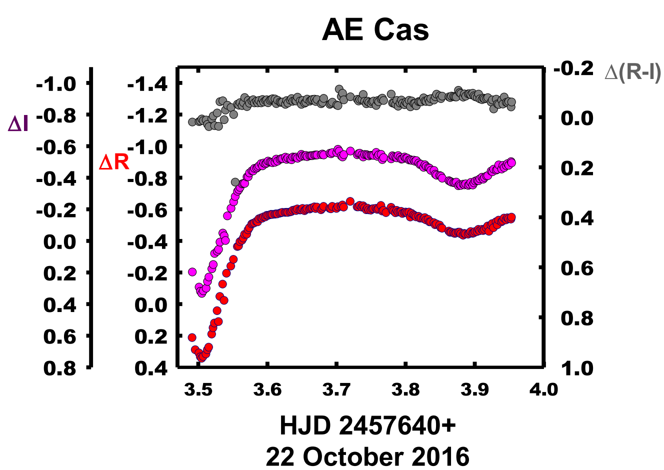

Figure 3. R_c, I_c, and R_c–I_c color curves on the night of 2016 October 22.

and catalog name ASASSN-V J012700.39+700738.1. It is given as Figure 2.

3. 2017 VR_cI_c Photometry

The present observations were taken with the DSO 0.81 m reflector at Philips Gap, North Carolina, on 2016 October 2, 3 and 23 (3.7–11.1 UT), inclusive, with a thermoelectrically

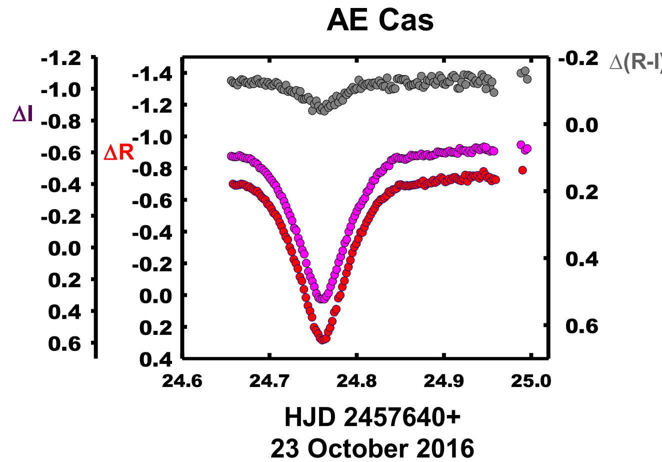

Figure 4. R_c, I_c, and R_c–I_c color curves on the night of 2016 October 23.

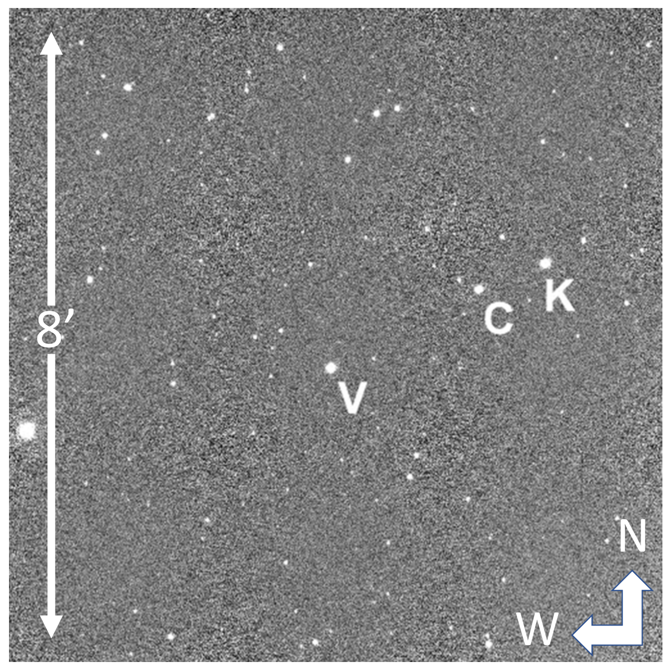

Figure 5. Finder chart; AE CAS (V), comparison star (C), and check (K).

cooled (−40°C) 2KX2K Apogee Alta by D. Caton with standard VR_cI_c filters and on October 23 (1.5–11.7 UT) with the 0.9 m reflector at Kitt Peak National Observatory (KPNO) remotely through the The Southeastern Association for Research in Astronomy (SARA) consortia with the liquid nitrogen (LN) cooled (−84.6°C) 2KX2K ARC-E2V42-40 chip camera by R. Samec.

Individual observations included 570 in *V*, 559 in R_c, and 531 in I_c. The probable error of a single observation was 9.9 mmag in *V*, 8.5 in R_c, and 9.6 in I_c. The nightly *C*–*K* values stayed constant throughout the observing run with a precision less than 1%. Exposure times varied from 20 to 80 s in *V*and 10–32 s in *R*and *I*. Figures 3 and 4 show light curves taken from 2016 October 22 and 23. Photometric targets are given in Table 1.

The variable (denoted as *V*), also designated TYC 4301 1388 1, NSVS 240090, has a position of [$\alpha(2000) = 01^h27^m00\overset{s}{.}3467$, $\delta(2000) = +82°03'44\overset{''}{.}4$ UCAC3: the USNO CCD Astrograph Catalog], $V = 12.70$–13.50 (2MASS), a parallax of 1.37 ±

Table 1
Photometric Targets

Star	Label	Name	V	J–K (2MASS)
Variable	V	AE CAS, TYC, 4301 1388 1, NSVS 240090	12.70–13.50	0.32 ± 0.02
Comparison	C	GSC 4301 1907, 3UC321-010572	12.68	0.260 ± 0.035
Check	K	GSC 4301 1549, 3UC345-013313	11.880	0.756 ± 0.046

Table 2
Photometric Observations of AE CAS

ΔV	VHJD 2457660+	ΔR_c	RcHJD 2457660+	ΔI_c	IcHJD 2457660+
0.214	3.4915	0.214	3.4915	0.199	3.4919
0.291	3.4961	0.291	3.4961	0.295	3.5017
0.311	3.5014	0.311	3.5014	0.321	3.5036
0.336	3.5034	0.336	3.5034	0.335	3.5056
0.345	3.5053	0.345	3.5053	0.318	3.5077
0.334	3.5074	0.334	3.5074	0.302	3.5119
0.318	3.5116	0.318	3.5116	0.259	3.5138
0.291	3.5136	0.291	3.5136	0.231	3.5158
0.275	3.5155	0.275	3.5155	0.179	3.5201

(This table is available in its entirety in machine-readable form.)

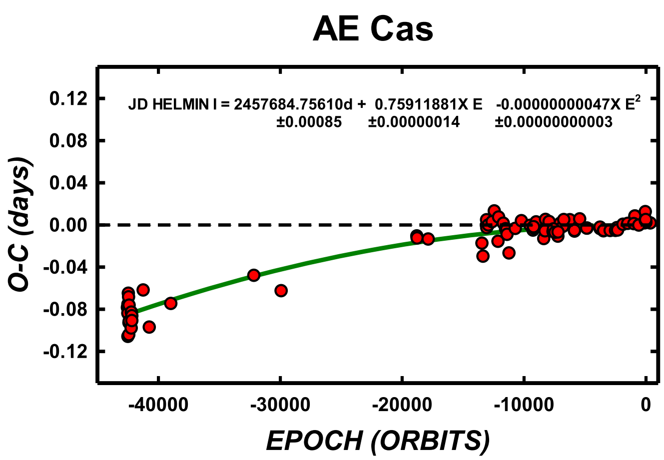

Figure 6. The period study of 89 yr indicates a continuous period decrease.

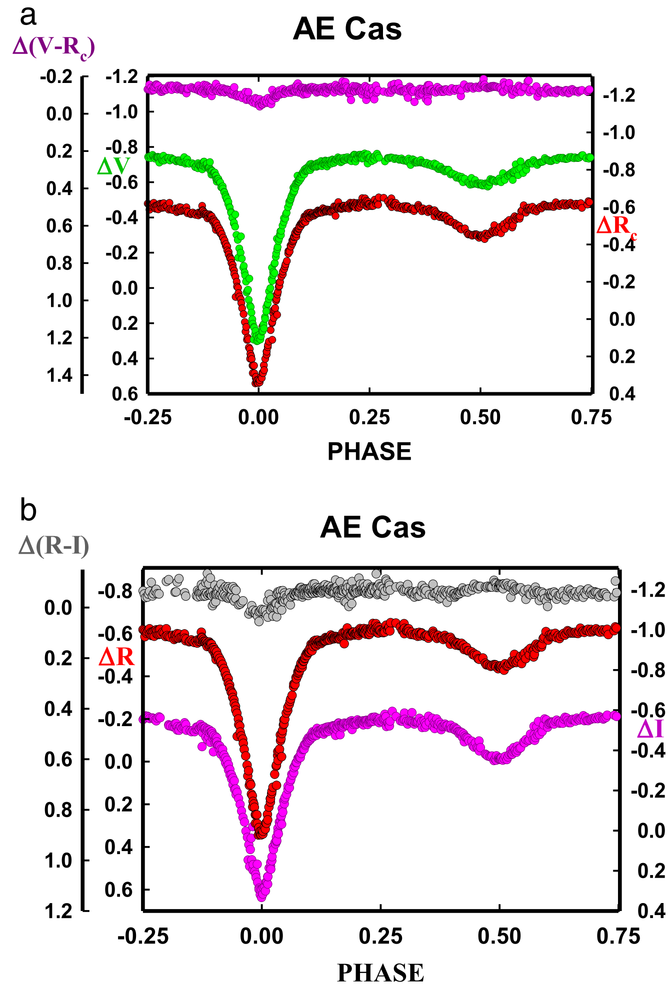

Figure 7. (a) V, R_c light curves and V–R color curves (variable comparison) with magnitudes phased with Equation (3). (b) R_c, I_c light curves and R_c–I_c color curves (variable comparison) with magnitudes phased with Equation (3).

0.05 mas, and a distance of 730 ± 20 pc (*Gaia*; Lindegren et al. 2018). The comparison star was denoted as C, and designated GSC 4301 1907 and 3UC321-010572 with a position of [$\alpha(2000) = 01^h27^m25^s.1189$, $\delta(2000) = +70°08'44''.861$ UCAC3]. The check star (denoted as K) is also designated as GSC 4301 1549 and has a position of [$\alpha(2000) = 01^h27^m36^s.11475$, $\delta(2000) = 70°09'6''.494$, UCAC3], $V = 11.880$, and a distance of 649 pc (2MASS).

The finder chart is given as Figure 5 with the variable star (V), comparison star (C), and check star (K) shown. Our observations are listed in Table 2, with differences in magnitude by filters ΔV, ΔR_c, and ΔI_c (variable star minus comparison star in each filter).

4. 89 yr Orbital Period Study

A total of 88 times of minimum light were used in our period study beginning with 14 timings by Hoffmeister (1940). Many of the subsequent timings were taken by the noted observer, Kurt Locher (1989a, 1989b, 1989c, 1990a, 1990b, 1991a, 1991b, 1992a, 1992b, 1992c, 1993a, 1993b, 1994, 1995, 1997a, 1997b, 1998a, 1998b, 2000a, 2000b, 2002a, 2002b, 2005 2007). These are listed in Table 3. Five times of minimum light were determined from our present observations, which include three primary eclipses and two secondary eclipses (with errors):

HJD Min I = 2457663.5055 ± 0.0005, 2457684.76093 ± 0.00005, 2457684.7616 ± 0.0001

HJD Min II = 2457663.8843 ± 0.0006, and 2457664.652.

In addition, eight observations at minima were introduced as low weighted times of minimum light taken from archived All-Sky Automated Survey for Supernovae Variable Star Catalog (ASAS) data and as well as a number of early visual observations (the amplitude of the primary eclipse is nearly 1 mag). This study covers an interval of some 89 yr of observations.

Table 3
$O - C$ Residual Calculations of AE CAS

	Epochs 2400000+	Cycles	Linear Residuals	Quadratic Residuals	Reference
1	25411.5000	−42514.0	−0.0037	0.0071	Hoffmeister (1940)
2	25424.4050	−42497.0	−0.0037	0.0071	Hoffmeister (1940)
3	25433.5090	−42485.0	−0.0092	0.0016	Hoffmeister (1940)
4	25436.5540	−42481.0	−0.0006	0.0101	Hoffmeister (1940)
5	25439.5600	−42477.0	−0.0311	−0.0204	Hoffmeister (1940)
6	25465.4110	−42443.0	0.0098	0.0204	Hoffmeister (1940)
7	25481.3490	−42422.0	0.0062	0.0168	Hoffmeister (1940)
8	25493.4590	−42406.0	−0.0297	−0.0191	Hoffmeister (1940)
9	25503.3390	−42393.0	−0.0183	−0.0077	Hoffmeister (1940)
10	25512.4650	−42381.0	−0.0017	0.0088	Hoffmeister (1940)
11	25525.3550	−42364.0	−0.0168	−0.0063	Hoffmeister (1940)
12	25644.5300	−42207.0	−0.0237	−0.0136	Hoffmeister (1940)
13	25650.6180	−42199.0	−0.0087	0.0015	Hoffmeister (1940)
14	25685.5340	−42153.0	−0.0123	−0.0022	Hoffmeister (1940)
15	25688.5660	−42149.0	−0.0167	−0.0067	Hoffmeister (1940)
16	26391.5390	−41223.0	0.0104	0.0186	Hoffmeister (1940)
17	26769.5450	−40725.0	−0.0257	−0.0185	Hoffmeister (1940)
18	28108.6530	−38961.0	−0.0067	−0.0028	Hoffmeister (1940)
19	34982.4860	−29906.0	−0.0123	−0.0203	Hoffmeister (1940)
20	33282.8335	−32145.0	0.0066	0.0009	Wood & Forbes (1963)
21	43435.3260	−18771.0	0.0179	0.0060	Srivastava & Kandpal (1984)
22	43454.3020	−18746.0	0.0159	0.0040	Srivastava & Kandpal (1984)
23	44144.3400	−17837.0	0.0131	0.0014	Srivastava & Kandpal (1984)
24	47491.2910	−13428.0	0.0007	−0.0090	Locher (1989a)
25	47557.3220	−13341.0	−0.0118	−0.0215	Locher (1989b)
26	47777.4960	−13051.0	0.0171	0.0077	Brno 30
27	47777.5010	−13051.0	0.0221	0.0127	Brno 30
28	47786.6030	−13039.0	0.0147	0.0053	Locher (1989c)
29	47885.2910	−12909.0	0.0170	0.0076	Locher (1990a)
30	48127.4530	−12590.0	0.0195	0.0104	Locher (1990b)
31	48260.3090	−12415.0	0.0293	0.0204	Locher (1991a)
32	48489.5340	−12113.0	−0.0001	−0.0089	Locher (1991b)
33	48533.5860	−12055.0	0.0229	0.0142	Locher (1992a)
34	48820.5270	−11677.0	0.0162	0.0078	Locher (1992b)
35	48963.2360	−11489.0	0.0105	0.0023	Locher (1992c)
36	49031.5560	−11399.0	0.0096	0.0015	Borovic'ka (1993)
37	49054.3250	−11369.0	0.0050	−0.0031	Locher (1993a)
38	49173.4890	−11212.0	−0.0129	−0.0209	Locher (1993b)
39	49561.4220	−10701.0	0.0093	0.0018	Locher (1994)
40	49948.5800	−10191.0	0.0157	0.0087	Locher (1995)
41	50488.3090	−9480.0	0.0099	0.0036	Locher (1997a)
42	50670.4930	−9240.0	0.0049	−0.0012	Locher (1997b)
43	50762.3480	−9119.0	0.0063	0.0004	Locher (1998a)
44	50863.3170	−8986.0	0.0122	0.0064	Locher (1998b)
45	51341.5460	−8356.0	−0.0049	−0.0099	Locher (1999)
46	51448.6000	−8215.0	0.0131	0.0082	Locher (2000a)
47	51672.5380	−7920.0	0.0105	0.0059	Locher (2000b)
48	52215.2940	−7205.0	−0.0049	−0.0085	Locher (2002a)
49	52366.3710	−7006.0	0.0071	0.0037	Locher (2002b)
50	52532.6150	−6787.0	0.0037	0.0005	Locher (2007)
51	52964.5600	−6218.0	0.0089	0.0066	Diethelm (2004)
52	53257.5690	−5832.0	−0.0027	−0.0045	Locher (2005)
53	53579.4470	−5408.0	0.0081	0.0069	Locher (2005)
54	54031.8730	−4812.0	−0.0019	−0.0022	Nelson (2007)
55	55894.7510	−2358.0	−0.0062	−0.0027	Diethelm (2004)
56	57973.9820	381.0	−0.0070	0.0016	ASAS
57	57696.9050	16.0	−0.0049	0.0030	ASAS
58	57362.8950	−424.0	−0.0018	0.0053	ASAS
59	57044.8270	−843.0	0.0018	0.0081	ASAS
60	57046.7180	−840.5	−0.0050	0.0013	ASAS
61	57619.0940	−86.5	−0.0061	0.0017	ASAS
62	57704.8750	26.5	−0.0057	0.0023	ASAS
63	57008.7690	−890.5	0.0020	0.0082	ASAS

Table 3
(Continued)

	Epochs 2400000+	Cycles	Linear Residuals	Quadratic Residuals	Reference
64	50708.4521	381.0	−0.0070	0.0016	Safar & Zejda (2000)
65	51423.5381	16.0	−0.0049	0.0030	Agerer & Hubscher (2001)
66	51913.9283	−424.0	−0.0018	0.0053	Nelson (2002)
67	51946.9524	−843.0	0.0018	0.0081	Nelson (2002)
68	52041.4595	−840.5	−0.0050	0.0013	Blaettler (2001)
69	52585.7598	−86.5	−0.0061	0.0017	Samolyk (2013)
70	52230.4804	26.5	−0.0057	0.0023	Brát et al. (2007)
71	53251.4967	−890.5	0.0020	0.0082	Hubscher et al. (2005)
72	54017.4498	−9190.0	0.0080	0.0020	Hubscher & Walter (2007)
73	54843.3705	−8248.0	0.0022	−0.0027	Lampens et al. (2010)
74	54843.3719	−7602.0	0.0004	−0.0038	Lampens et al. (2010)
75	55060.4764	−7558.5	0.0027	−0.0014	Hubscher et al. (2010)
76	55073.3818	−7434.0	−0.0007	−0.0047	Hubscher et al. (2010)
77	55473.4374	−6717.0	0.0100	0.0070	Hubscher (2011)
78	55804.4133	−7185.0	−0.0009	−0.0045	Hubscher & Lehmann (2012)
79	55940.2959	−5840.0	−0.0020	−0.0039	Marino (2012)
80	56274.3137	−4831.0	−0.0018	−0.0022	Hubscher (2014)
81	56567.3344	−3743.0	−0.0045	−0.0032	Hubscher (2014)
82	56949.5505	−3743.0	−0.0031	−0.0018	Hubscher (2015)
83	57260.4082	−3457.0	−0.0071	−0.0054	Hubscher (2016)
84	57663.5055	−28.0	−0.0031	0.0047	Present Observations
85	57663.8843	−27.5	−0.0039	0.0040	Present Observations
86	57664.6518	−26.5	0.0045	0.0124	Present Observations
87	57684.7609	0.0	−0.0031	0.0048	Present Observations
88	57684.7616	0.0	−0.0024	0.0055	Present Observations

(This table is available in machine-readable form.)

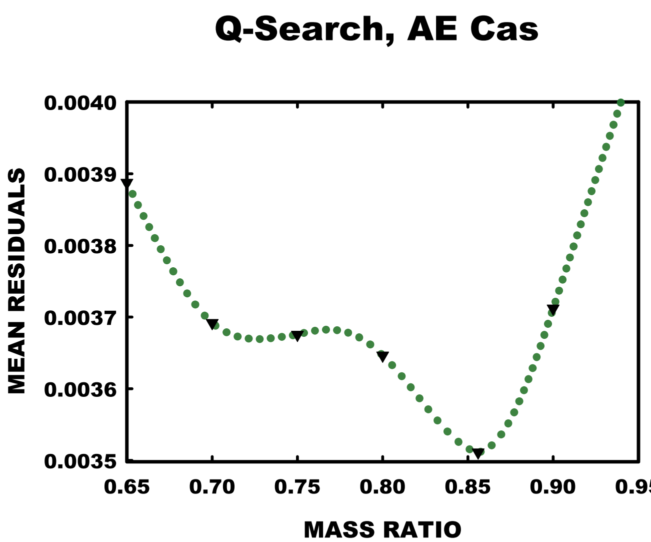

Figure 8. Mass ratio search conducted with a number of solutions which minimized at ∼0.86.

The following linear and quadratic ephemerides were determined from the times of minimum light:

$$\text{JD Hel Min I} = 2457684.7640 \pm 0.0013\text{d} + 0.75912076 \pm 0.00000008\text{E} \tag{3}$$

$$\text{JD Hel Min I} = 2457684.7561 \pm 0.0013\text{d} + 0.75911881 \pm 0.00000022\text{E} - 0.000000000048 \pm 0.000000000004\text{E}^2. \tag{4}$$

The $O-C$ quadratic and linear residual calculations are given in Table 3. The plot of the quadratic residuals are displayed in Figure 6. The quadratic term is statistically significant at about $\sim 11\sigma$. This ephemeris yields a $\dot{P} = -4.62 \pm 0.014 \times 10^{-8}$ day(yr)$^{-1}$ or a mass exchange rate of $\frac{dM}{dt} = \frac{\dot{P}M_1M_2}{3P(M_1 - M_2)} = (-1.52 \pm 0.54) \times 10^7$ Myr^{-1} in a conservative scenario. These are typical rates of magnetic braking (Qian et al. 2017).

This 89 yr trend is probably due to magnetic braking for this solar-type binary. A continuance of this trend would lead to the formation of a W UMa binary and ultimately the system would become unstable, resulting in a red novae event and finally a single fast-rotating spectrally bluer star (Tylenda & Kamiński 2016). Alternately, the period change could be a part of a long sinusoidal variation due to the presence of a distant third body. However, third-light iterations resulted in nonphysical, negative values in the synthetic light-curve calculation.

5. Light Curves

The VR_cI_c phased light curves calculated from Equation (3) are shown in Figures 7(a) and (b). Light-curve magnitude means at quarter phases are given in Table 4. The O'Connell effect, an indicator of spot activity, is negligible. For a solar-type binary such as this, that does not mean that there is no magnetic activity. Likely, the surface is saturated with magnetic activity but is averaging out in flux level, so the light curves are not a good means of detecting magnetic phenomena. The differences in minima are large, 0.67–0.86 mag from I_c to V, probably indicating noncontact light curves. The amplitudes of

Table 4
Light-curve Characteristics for AE CAS

Filter	Phase	Mag	Phase	Mag
		Min I		Max I
	0.0		0.25	
V		0.279 ± 0.018		− 0.739 ± 0.016
R		0.331 ± 0.013		− 0.617 ± 0.012
I		0.309 ± 0.019		− 0.551 ± 0.008
		Min II		Max II
Filter	Phase	Mag	Phase	Mag
	0.5		0.75	
V		− 0.586 ± 0.005		− 0.738 ± 0.004
R		−0.443 ± 0.008		− 0.611 ± 0.014
I		− 0.358 ± 0.007		− 0.565 ± 0.008
Filter	Min I–Max I		Filter	Min I–Min II
V	1.018 ± 0.034		V	0.865 ± 0.023
R	0.947 ± 0.025		R	0.773 ± 0.020
I	0.860 ± 0.027		I	0.666 ± 0.026
Filter	Max I–Max II		Filter	Min II–Max I
V	0.001 ± 0.020		V	0.153 ± 0.021
R	0.006 ± 0.026		R	0.174 ± 0.020
I	− 0.014 ± 0.016		I	0.193 ± 0.015

the light curves are 0.86–1.02 mag in I_c to V indicating a fairly high inclination and high mass ratio for the binary. The V–I_c and R–I_c color curves fall at phase 0.0, which is characteristic of a contact binary, however the color curves rise slightly at phase 0.5, which indicates that the secondary component is underfilling its Roche lobe. Thus, the shape of the curves indicates a near-contact semi-detached binary coming into contact.

6. Temperature

2MASS gives $J–K = 0.320 \pm 0.053$ for the binary. The APASS-DR9 gives $B–V = 0.53$. These correspond to an ~F7 ± 2V eclipsing binary which yields a temperature of 6250 ± 300 K. Fast-rotating binary stars of this type are noted for having convective atmospheres, so spots are expected.

7. Light-curve Solution

The V, R_c, and I_c curves were pre-modeled with binary maker 3.0 (Bradstreet & Steelman 2002) and fits were determined in the three filter bands. The result of the best hand-fit was that of a classical Algol eclipsing binary with fill outs of 85% and 100%. This would indicate in themselves, that the Roche Lobes of the secondary component was filling while the primary component was underfilling its critical surface. The parameters were then averaged and input into a three-color simultaneous light-curve calculation using the 2016 Wilson–Devinney (W–D) Program (Wilson & Devinney 1971; Wilson 1990, 1994, 2008, 2012; Van Hamme & Wilson 1998, 2007; Wilson et al. 2010; Wilson & Van Hamme 2014). Convective parameters $g = 0.32$ and $A = 0.5$ were used. The solution was computed in Mode 2 in order to calculate the best configuration and it converged to a solution in a detached mode with no indication that one should change modes (Mode 5 is the classical Algol with the primary underfilling its critical Roche lobe and the secondary filling its critical lobe. Mode 4 is opposite, with the primary underfilling and the secondary critically filling.)

The eclipses were not total, so a mass ratio search (q-search) was conducted converging on the original solution with a high mass ratio of 0.86. The q-search is graphed in Figure 8 and the solution is given as Table 5.

This result is not definitive, but a radial velocity curve is needed for certainty. The normalized V and the R_c, I_c light

Table 5
V, R_c, I_c W–D Program Solution Parameters

Parameters	Values
$\lambda_V, \lambda_R, \lambda_I$(nm)	550, 640, 790
g_1, g_2	0.32
A_1, A_2	0.5
Inclination (°)	75.88 ± 0.03
T_1, T_2 (K)	6250, 4189 ± 1
Ω_1, Ω_2	4.2186 ± 0.0026, 3.5435 ± 0.0020
$q(m_2/m_1)$	0.8560 ± 0.0005
Fill outs: F_1, F_2 (%)	83.1969 ± 0.0005, 99.0737 ± 0.0006
$L_1/(L_1+L_2+L_3)_I$	0.7808 ± 0.0004
$L_1/(L_1+L_2+L_3)_R$	0.8279 ± 0.0008
$L_1/(L_1+L_2+L_3)_V$	0.8789 ± 0.0007
JD_o (days)	2457684.76120 ± 0.00010
Period (days)	0.759141 ± 0.000008
r_1/a, r_2/a (pole)	0.2941 ± 0.0017, 0.3389 ± 0.0016
r_1/a, r_2/a (point)	0.3180 ± 0.0023, 0.4386 ± 0.0097
r_1/a, r_2/a (side)	0.3014 ± 0.0018, 0.3547 ± 0.0020
r_1/a, r_2/a (back)	0.3113 ± 0.0021, 0.3840 ± 0.0029

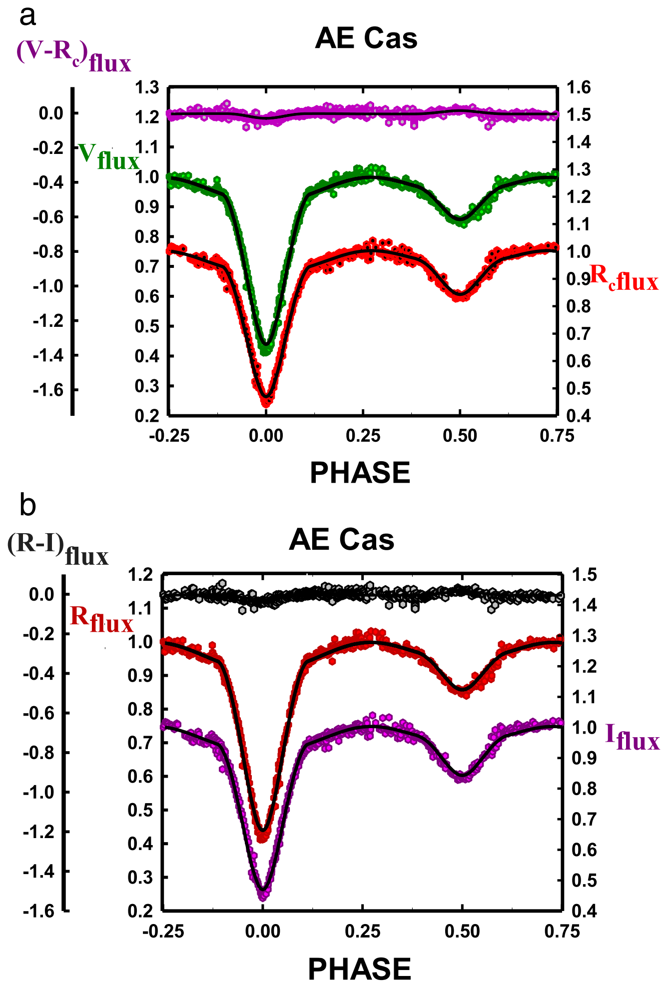

Figure 9. (a) V, R_c normalized fluxes and the B–V color curves overlaid by the detached solution for AE CAS. (b) R_c, I_c normalized fluxes and the B–V color curves overlaid by the detached solution of AE CAS.

curves with the detached solution curves overlain are displayed in Figures 9(a) and (b). The Roche lobe surfaces are given in Figures 10(a)–(d).

8. Discussion

AE Cas is a dwarf solar-type binary in an unusual but a very nearly classical Algol-type configuration. The synthetic light curve determined fill outs of the primary and secondary components were 83% and 99%, respectively. This configuration could result after a set of evolutionary mass exchanges called the Algol paradox. However, the process was evidently sped up by magnetic braking. Otherwise this process would probably take longer than the age of the universe for the formation of such a pre-W UMa binary. Its J–K color index indicates a surface temperature of $\sim$6250 K for the primary component. The secondary component has a temperature of $\sim$4200 K (K6V), which means that it is over-massive as compared to a single main-sequence star of this temperature. The light-curve solution mass ratio is $\sim$0.86 rather than the expected $\sim$0.54. However, the Algol paradox specifies that mass exchanges have been made between components so masses should not match main-sequence counter parts. We note that the photometric q determinations are only estimates of the physical mass ratio and masses obtained by a thorough radial

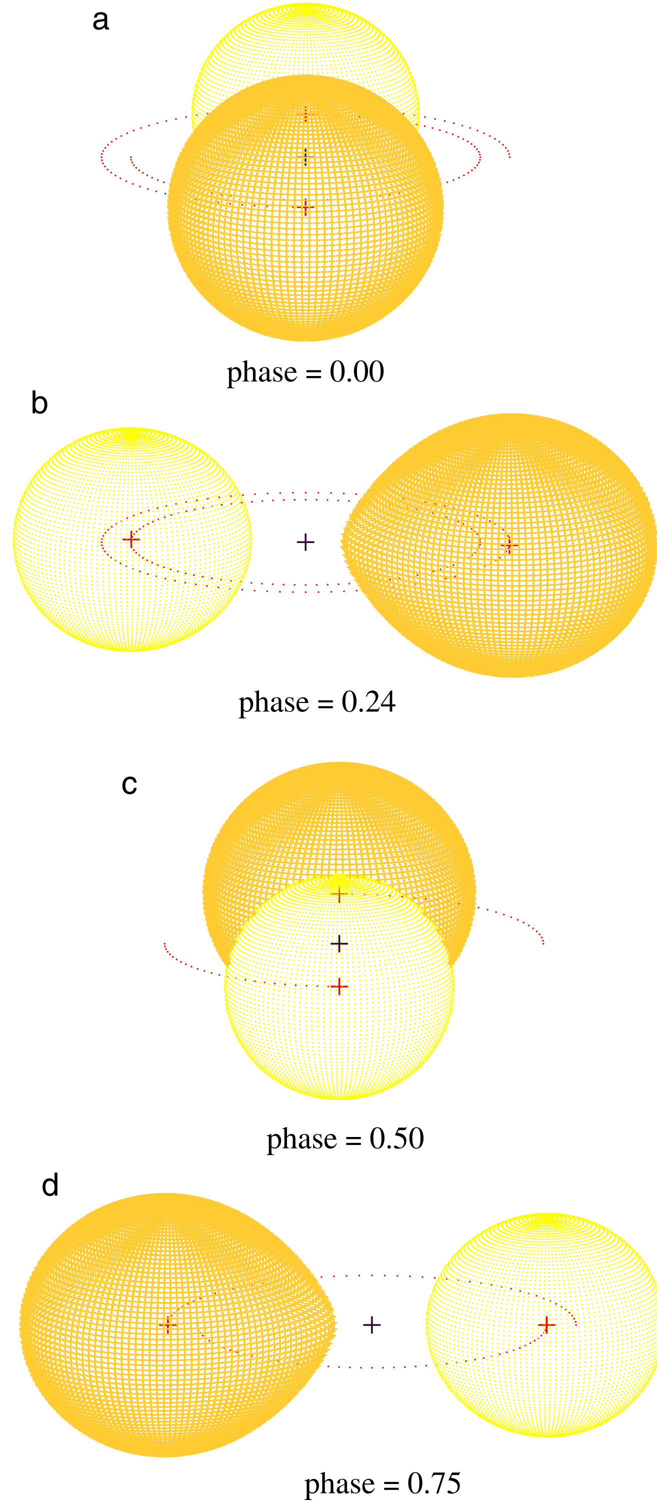

Figure 10. (a) Geometrical representation at phase 0.00 of AE CAS. (b) Geometrical representation at phase 0.25 of AE CAS. (c) Geometrical representation at phase 0.50 of AE CAS. (d) Geometrical representation at phase 0.75 of AE CAS.

velocity study. The inclination is 76° so the eclipses are partial. No spots (asymmetries) were discernible.

9. Conclusion

The period study of this pre-contact W UMa binary has an 89 yr time duration. The period is found to be continually decreasing at a high level of confidence. This is expected for a solar-type binary undergoing magnetic braking. This could be also due to a mass transfer from the primary component onto the secondary, which seems untenable for the configuration. The magnetic braking scenario will result in contact and then overcontact into an A-type W UMa binary. Continued magnetic braking will cause the system to slowly coalesce. This is due to loses in angular momentum from ion winds moving radially outward on stiff magnetic field lines rotating with the binary (out to the Alfvén radius). Ultimately, one would expect that the binary will become a rather normal, fast-rotating single A7V-type field star after a red novae coalescence event (with a ∼5% mass loss; Tylenda & Kamiński 2016). Of course, radial velocity curves are needed to confirm this proposed scenario and to obtain absolute (not relative) system parameters.

This work has made use of data from the European Space Agency (ESA) mission *Gaia* (https://www.cosmos.esa.int/gaia), processed by the *Gaia* Data Processing and Analysis Consortium (DPAC; https://www.cosmos.esa.int/web/gaia/dpac/consortium). Funding for the DPAC has been provided by national institutions, in particular the institutions participating in the *Gaia* Multilateral Agreement.

ORCID iDs

Ronald G. Samec https://orcid.org/0000-0002-4965-3542

References

Agerer, F., & Hubscher, J. B. 2001, IBVS, 5016, 2
Blaettler, E. 2001, BBSAG, 125, 3
Borovic'ka, J. 1993, IBVS, 3877, 3
Brát, L., Zejda, M., & Svoboda, P. 2007, OEJV, 0074, 1
Bradstreet, D. H., & Steelman, D. P. 2002, BAAS, 34, 1224
Chamberlain, H., Samec, R., Caton, D. B., & Faulkner, D. R. 2019, BAAS, 51, 4
Diethelm, R. 2004, IBVS, 5543, 3
Hoffmeister, C. 1928, AN, 234, 33
Hoffmeister, C. 1940, KVeBB, 5, 3.1
Hubscher, J. 2011, IBVS, 5984, 3
Hubscher, J. 2014, IBVS, 6118, 4
Hubscher, J. 2015, IBVS, 6152, 3
Hubscher, J. 2016, IBVS, 6157, 3
Hubscher, J., & Lehmann, P. B. 2012, IBVS, 6026, 4
Hubscher, J., Lehmann, P. B., Monninger, G., Steinbach, H.-M., & Walter, F. 2010, IBVS, 5941, 2
Hubscher, J., Paschke, A., & Walter, F. 2005, IBVS, 5657, 4
Hubscher, J., & Walter, F. 2007, IBVS, 5761, 2
Kochanek, C. S., Shappee, B. J., Stanek, K. Z., et al. 2017, PASP, 129, 104502
Kopal, Z. 1982, Ap&SS, 81, 123
Lampens, P., Kleidis, S., Van Cauteren, P., et al. 2010, IBVS, 5933, 2
Lindegren, L., Hernández, J., Bombrun, A., et al. 2018, A&A, 616A, 2
Locher, K. 1989a, BBSAG, 90, 3
Locher, K. 1989b, BBSAG, 91, 4
Locher, K. 1989c, BBSAG, 93, 3
Locher, K. 1990a, BBSAG, 93, 3
Locher, K. 1990b, BBSAG, 96, 2
Locher, K. 1991a, BBSAG, 97, 4
Locher, K. 1991b, BBSAG, 98, 3
Locher, K. 1992a, BBSAG, 99, 3
Locher, K. 1992b, BBSAG, 101, 3
Locher, K. 1992c, BBSAG, 102, 3
Locher, K. 1993a, BBSAG, 103, 2
Locher, K. 1993b, BBSAG, 104, 2
Locher, K. 1994, BBSAG, 107, 3
Locher, K. 1995, BBSAG, 110, 5
Locher, K. 1997a, BBSAG, 114, 5
Locher, K. 1997b, BBSAG, 115b, 2
Locher, K. 1998a, BBSAG, 116, 6
Locher, K. 1998b, BBSAG, 117, 4
Locher, K. 1999, BBSAG, 121, 4
Locher, K. 2000a, BBSAG, 121, 4
Locher, K. 2000b, BBSAG, 121, 2
Locher, K. 2002a, BBSAG, 127, 2
Locher, K. 2002b, BBSAG, 128, 2
Locher, K. 2005, OEJV, 3, 1
Locher, K. 2007, IBVS, 5438, 4
Marino, G. 2012, IBVS, 6033, 3, https://konkoly.hu/pub/ibvs/6001/6033.pdf
Nelson, R. H. 2002, IBVS, 5224, 1
Nelson, R. H. 2007, IBVS, 5701, 2
Qian, S.-B., He, J.-J., Zhang, J., et al. 2017, RAA, 17, 087
Russell, H. N., & Merrill, J. E. 1952, Contributions from the Princeton University Observatory (Princeton, NJ: Princeton Univ. Observatory)
Safar, J., & Zejda, M. 2000, IBVS, 4887, 2
Samolyk, G. 2013, Javso, 41, 122
Shappee, B. J., Prieto, J. L., Grupe, D., et al. 2014, ApJ, 788, 48
Srivastava, J. B., & Kandpal, C. D. 1984, A&A, 34, 281
Tylenda, R., & Kamiński, T. 2016, A&A, 592, A134
Van Hamme, W., & Wilson, R. E. 1998, BAAS, 30, 1402
Van Hamme, W., & Wilson, R. E. 2007, ApJ, 661, 1129
Wilson, R. E. 1979, ApJ, 234, 1054
Wilson, R. E. 1990, ApJ, 356, 613
Wilson, R. E. 1994, PASP, 106, 921
Wilson, R. E. 2008, ApJ, 672, 575
Wilson, R. E. 2012, AJ, 144, 73
Wilson, R. E., & Devinney, E. J. 1971, ApJ, 166, 605
Wilson, R. E., & Van Hamme, W. 2014, ApJ, 780, 151
Wilson, R. E., Van Hamme, W., & Terrell, D. 2010, ApJ, 723, 1469
Wood, D. B. 1971, AJ, 76, 701
Wood, D. B., & Forbes, J. E. 1963, AJ, 68, 257